

Malvidin attenuates behavioral and inhibits the TNF- α /Caspase-3/Nrf-2 expression in rotenone-induced Parkinson's disease in rats: insights from molecular docking

I. KAZMI¹, F.A. AL-ABBASI¹, N.A.R. ALMALKI^{1,2}, R.A. SHEIKH^{1,2}, S.D. AL-QAHTANI³, M.S. NADEEM¹, S. BEG⁴, M. AFZAL⁵

¹Department of Biochemistry, Faculty of Science, King Abdulaziz University, Jeddah, Saudi Arabia

²Experimental Biochemistry Unit, King Fahd Medical Research Center, King Abdulaziz University, Jeddah, Saudi Arabia

³Department of Medical Laboratory Sciences, College of Applied Medical Sciences, Majmaah University, Al Majmaah, Saudi Arabia

⁴Department of Pharmaceutics, School of Pharmaceutical Education and Research, Jamia Hamdard, Hamdard University, New Delhi, India

⁵Department of Pharmaceutical Sciences, Pharmacy Program, Batterjee Medical College, Jeddah, Saudi Arabia

S. Beg has designated the affiliation when this work was performed

Abstract. – OBJECTIVE: Malvidin is a natural, biologically active polyphenol found in several fruits. It exhibits several therapeutic benefits; however, limited studies are available on its effects on neurodegenerative clinical conditions, including Parkinson's disease. The study aimed to investigate the therapeutic properties of malvidin on rotenone-triggered Parkinson's disease in an animal model.

MATERIALS AND METHODS: To determine the effects of malvidin, rotenone (1.5 mg/kg) was injected subcutaneously into Wistar rats for 21 days, followed by a dose of malvidin (200 and 100 mg/kg). Behavioral tests were performed on the experimental animals before sacrifice. On the 22nd day of the experiment, biochemical tests were performed, including superoxide dismutase (SOD), glutathione (GSH), malondialdehyde (MDA), and catalase (CAT). The activity of neurotransmitters and their metabolites, including acetylcholine (ACh), acetylcholinesterase (AChE), dopamine (DA), norepinephrine (NE), serotonin (5-HT), 3,4-dihydroxyphenylacetic acid (DOPAC), homovanillic acid (HVA), and 5-hydroxyindoleacetic acid (5-HIAA) along with neuroinflammatory markers including interleukin-6 (IL-6), interleukin-1 β (IL-1 β), tumor necrosis factor- α (TNF- α), and nuclear factor erythroid 2-related factor 2 (Nrf-2) were estimated. Moreover, the level of the apoptotic marker, caspase-3, was also estimated. In addition, molecular docking was performed.

RESULTS: The administration of rotenone resulted in oxidative stress, cholinergic imbalances, dopaminergic alternations, and increased expression of inflammatory compounds. The docking analysis revealed that malvidin displayed a favorable binding affinity for AChE, showcasing a binding energy of -9.329 Kcal/mol.

CONCLUSIONS: The investigation concludes that malvidin exhibits neuroprotective effects due to its curative effects against inflammation and oxidative stress. These findings suggest that malvidin possesses therapeutic potential against rotenone-triggered behavioral, oxidative, and inflammatory abnormalities in rodents.

Key Words:

Antioxidant markers, Behavioral paradigms, Malvidin, Rotenone, Parkinson's disease.

Introduction

Parkinson's disease (PD) is a sluggishly developing neurological condition affecting nearly 1.5% to 2.0% of elderly people worldwide¹. PD is a devastating neurodegenerative disease that is symptomatized by neuronal degeneration, which causes motor abnormalities that impair movement and speech. Patients with PD experience

tremors and muscular rigidity due to the degenerative effects of the disease on dopaminergic neurons located in the central nervous system (CNS)^{2,3}. The pathophysiology of PD is linked with genetic and environmental causes, as well as inflammation, alterations, and mitochondrial malfunction, which have an impact on the onset and progression of PD⁴.

Rotenone is a plant-based crystalline isoflavone mostly used as a pesticide and insecticide in agriculture. Rotenone causes dopaminergic neurodegeneration by affecting the functionality of mitochondrial complex I⁵. Rotenone has an affinity for mitochondrial complex I, and by binding, rotenone disturbs the electron transport chain. Rotenone accumulates α -synuclein in the brain and has a lipophilic nature that allows it to penetrate the blood-brain barrier^{6,7}. In addition, rotenone affects superoxide generation in activated microglia. Thus, rotenone has frequently been included in the development of clinically relevant research models of PD⁸.

Oxidative stress is a primary characteristic of neurodegenerative disorders. Reversing oxidative stress has been considered to be beneficial in the treatment of PD⁹. Similarly, mitochondrial injury is vital in the onset of PD, and preserving mitochondrial function has been shown to be effective in treating neurodegeneration¹⁰. Neuroinflammation is critical in the pathogenesis of PD, and it has been discovered that reducing neuroinflammation has a neuroprotective effect¹¹. Oxidative stress and neuroinflammation inhibit the kinase cascade, which includes protein kinase B.

Moreover, neurodegeneration advanced as a consequence of phosphoinositide 3-kinase (PI3K) and mammalian target of rapamycin (mTOR), fostering oxidative damage and inflammation within neural tissue¹².

Malvidin is an anthocyanidin with several medicinal properties that confer many health benefits. Anthocyanidins are plant-derived phenolic compounds mostly found in greens and fruits¹³. Malvidin has been proven to be an effective anti-stress molecule, reducing oxidative stress¹⁴. Additionally, malvidin has anticancer properties and arrests the cell cycle by controlling the phosphorylation of signal transducer and activator of transcription 3 (STAT3)¹⁵. Moreover, malvidin has been proven to be beneficial in the management of neurological disorders such as Alzheimer's disease (AD). It was reported to reduce tau protein aggregation by activating FK506 binding protein 52 (FKBP52), improving AD treatment¹⁶.

Furthermore, anthocyanins, such as malvidin, have been shown to slow the progression of certain disorders owing to their anti-inflammatory and antioxidative properties¹⁷.

Despite advances in the medical sector and research, there is no accurate treatment for PD. Extensive research is being conducted on neurodegenerative disorders worldwide; however, no complete prophylaxis or cure has been discovered for PD. Current treatments for PD only provide short-term relief to patients by replacing existing DA, and do not completely stop the degeneration of neurons¹⁸. Therefore, the development of preventive strategies for chronic neural clinical conditions is required. Although studies^{19,21} have been conducted to determine the neuroprotective properties of certain plant-based compounds with anti-inflammatory properties, interventions without adverse effects are warranted. The current work aims to determine the neuroprotective efficacy of malvidin in a rotenone-triggered PD experimental rodent model.

Materials and Methods

Chemicals and Reagents

Rotenone (Sigma-Aldrich, St. Louis, MO, USA) was employed in the research. The investigative kits for interleukins beta (IL-1 β), IL-6, tumor necrosis factor α (TNF- α), nuclear factor erythroid 2-related factor 2 (Nrf-2), and caspase-3 were dignified by using a rat enzyme-linked immunosorbent assay (ELISA) kit and malvidin ($\geq 95.0\%$) was obtained from MSW Pharma (Chandrapur, Maharashtra, India).

Animals

Male Wistar rats aged 10-12 weeks (180 \pm 20 g) were included in this study. All rodents were housed in a propylene cage for one week prior to the experiment. The temperature was adjusted at 24 \pm 5 $^{\circ}$ C, whereas humidity was set at 50-60% with 12 hours of alternate light and dark cycle. Proper animal food (pellets) and fresh drinking water were supplied to all the experimental subjects. The Committee for the Purpose of Control and Supervision of Experiments on Animals (CPCSEA) guidelines were strictly followed while the experiments were being performed. The work was approved by the Institutional Animal Ethics Committee (IAEC/TRS/PT/023/029), date-08/09/2023 and research was conducted as per the Animal Research: Reporting of In Vivo Experiments (ARRIVE) guidelines²².

Experimental Design

The rodents were separated into four groups (n=6). The first group received only sunflower oil and was labelled the “control group,” while the second group was (Rotenone control) administered 0.5 mg/kg of rotenone. The third group was named the low-dose treatment group (Rotenone 0.5 mg/kg + 100 mg/kg malvidin), and the fourth group was the high-dose treatment group (Rotenone 0.5 mg/kg + 200 mg/kg malvidin). Except for the control group, each group was provided 0.5 mg/kg of rotenone *via* a subcutaneous route for three weeks. The high- and low-dose groups were provided 200 mg/kg and 100 mg/kg malvidin for 21 days, respectively, one hour before rotenone injection. A behavioral test was conducted on all experimental rodents 24 hours after the last dose of rotenone. Immediately after completing the behavioral test, all the animals were sacrificed, and the brain from each animal was dissected, washed using cold saline, and preserved at 4°C in formalin solution.

Behavioral Study

Catalepsy test

The catalepsy measurement was performed with a wooden box with proportions of 25 cm × 20 cm × 35 cm (height × width × length) accompanied by a 20 cm long horizontal bar with a diameter of 0.8 cm hanging 9 cm above the base made of stainless steel. The rats were positioned on the bar in a half-rearing mode, and a catalepsy score was recorded²³.

Open field test

The experiment was accomplished in a rectangular frame. The frame floor was made of cloth and divided into 25 squares of dimensions 20 × 20 (length × width). The locomotor activity of the rats was observed by placing an animal in a square at the center of the floor. Motor parameters were examined, including the duration spent in the initial place, rearing, distance covered by a rat, and entries in the central square. Finally, overall activity was calculated²⁴.

Rota-rod test

The rota-rod experiment assessed the coordination and motor balance of the animals, as described in an earlier study²⁵. Each rat was mounted on a rod (diameter=7 cm) and a rotational speed of 5 rpm, and the sustained duration

was recorded using a 3-minute maximum cut-off latency.

Biochemical analyses

Phosphate buffer was used to prepare the brain tissue homogenate, and the supernatant was obtained by centrifugation of the mixture for 25 min (15,000-25,000 rpm). The clear supernatant was used for biochemical analyses.

Superoxide dismutase (SOD)

SOD activity was estimated according to a previously described protocol²⁶. In this assay, xanthine generates superoxide. The supernatant was aliquoted and incubated after being placed in a test tube containing xanthine, nitroblue tetrazolium (NBT), and phosphate buffer. SOD activity was determined as units per mL (U/mL) and measured at 560 nm using a spectrophotometer.

Catalase (CAT)

In a test tube, 500 L of homogenate supernatant was added to a mixture of hydrogen peroxide (1,000 µL) and phosphate buffer (2,000 µL). The mixture was transferred to a cuvette, and spectrophotometric analysis was conducted at 240 nm for 30 s. Catalase expression was measured as the number of U/mL^{27,28}.

Reduced glutathione (GSH)

GSH was analyzed as per the previously described method²⁹. A mixture of 100 µL of homogenate, 10% of C₂HCl₃O₂ (trichloroacetic acid), and Ellman's reagent was prepared in a reaction tube and centrifuged at 2,000 rpm for the duration of 15 minutes. Spectrophotometric observations were noted at a wavelength of 412 nm. The output was represented as U/mg.

Malonaldehyde (MDA)

MDA was estimated as a lipid peroxidation marker as per a previously described method^{30,31}. The brain tissue homogenate was mixed with acetic acid (20%), thiobarbituric acid (8%), and dodecyl sulfate (0.8%). The tube was then heated for 60 minutes at 90°C to boil the mixture. After cooling, the mixture was submitted for centrifugation for 15 minutes at 1,500-2,000 rpm. Readings were taken at 532 nm, and MDA activity was represented as mmol/L.

Neurotransmitter estimation

The levels of neurotransmitters such as norepinephrine (NE), dopamine (DA), serotonin (5-

HT) and their metabolites, 5-hydroxyindoleacetic acid (5-HIAA), homovanillic acid (HVA) and 3,4-dihydroxyphenylacetic acid (DOPAC) were estimated by the HPLC (High-performance liquid chromatography, Agilent 1100, Agilent Technologies Helwette-Packard-Strasse 876337, Waldbronn, Germany) technique. The brain tissue samples were homogenized in 0.17 M perchloric acid. Using a reversed-phase liquid chromatography system with electrochemical detection, supernatants from tissue homogenates were injected directly into the chromatography system in a 20 μ l volume.

ACh expression in the brain was estimated as per a previously described method³². Enzyme inactivation was performed by boiling tissue samples to release ACh. A brown compound was formed by the reaction of ACh with ferric chloride, which was measured at 540 nm using a blank. The ACh level was determined as μ mol/g of tissue. The AChE was estimated in tissue as per the protocol described by Haider et al³³, and its activity was measured as U/mg in brain tissue.

Neuroinflammatory Assay

The supernatant was used as a reagent to estimate the cytokine activity of TNF- α , IL-1 β , and IL-6 using a kit as per the manufacturer's guidelines. The concentration of TNF- α , IL-1 β , and IL-6 were measured in pg/mL. Similarly, Nrf-2 and caspase-3 expression in the brain tissue homogenate were estimated by ELISA as per the protocol provided in the kit manual. The concentration of Nrf-2 and caspase-3 expression was measured in ng/mL.

Molecular Docking

The amino acid sequences and three-dimensional X-ray crystallographic structures of the amino acid sequences and three-dimensional X-ray crystallographic structures AChE, ChAT, TNF- α , IL-6, IL-1 β , caspase-3, and Nrf-2 were retrieved from the NCBI and Protein Data Bank (PDB), respectively. A BLAST search was conducted within the PDB to identify analogous sequences. For molecular docking, side chains for each protein were generated using CHIMERA v1.16, followed by optimization procedures comprising 1000 Steepest Descent steps with a 0.1 Å Steepest Descent size, the addition of hydrogen atoms, and setting protonation states for histidine residues. Subsequently, non-standard residues, water molecules, and extraneous chains were eliminated using the Biovia Dis-

covery Studio Visualizer V21.1.0.20298 (Biovia Discovery Studio Visualize). The receptor grid was determined through the combined use of AutoDock Vina 1.2.5 (Scripps Research Institute, La Jolla, CA, USA), Chimera (University of California, San Francisco, CA, USA) and Maestro (Schrödinger, LLC, New York, NY, USA). Ligands and the target molecule malvidin were prepared using MarvinSketch v21.13, followed by cleaning using the MMFF94 force field. The lowest energy conformers were saved in a 3D mol2 file format. AutoDock Vina 1.2.5 was employed for molecular docking, and the resulting data were visualized using Biovia Discovery Studio.

Statistical Analysis

The study employed a one-way ANOVA to analyze data presented as standard error of the mean (SEM) obtained using GraphPad Prism version 8.0.2 (Boston, MA, USA). Data normality was verified using the Shapiro-Wilk test. Significant differences between groups were assessed with Tukey's post hoc test following a significant one-way ANOVA ($p < 0.05$).

Results

Behavioral Tests

Catalepsy test

The duration of catalepsy was significantly extended in rotenone-induced rats ($p < 0.001$) than in control animals. The experimental groups that received 100 and 200 mg/kg malvidin depicted a decrease [F (3, 20)=10.87, $p = 0.0002$] in catalepsy duration collated to the animals treated with rotenone (Figure 1A).

Open-field test

The open field activity showed significant deprivation ($p < 0.001$) in the animals injected with rotenone than the control group. However, the open field test activity was successfully recovered [F (3, 20)=11.45, $p = 0.0001$] in both experimental groups treated with malvidin (100 and 200 mg/kg) as compared to rotenone-induced rats (Figure 1B).

Rotarod test

In the rotarod test, the rotenone-induced behavioral alterations in rats were attenuated by malvidin treatment. The retention time was re-

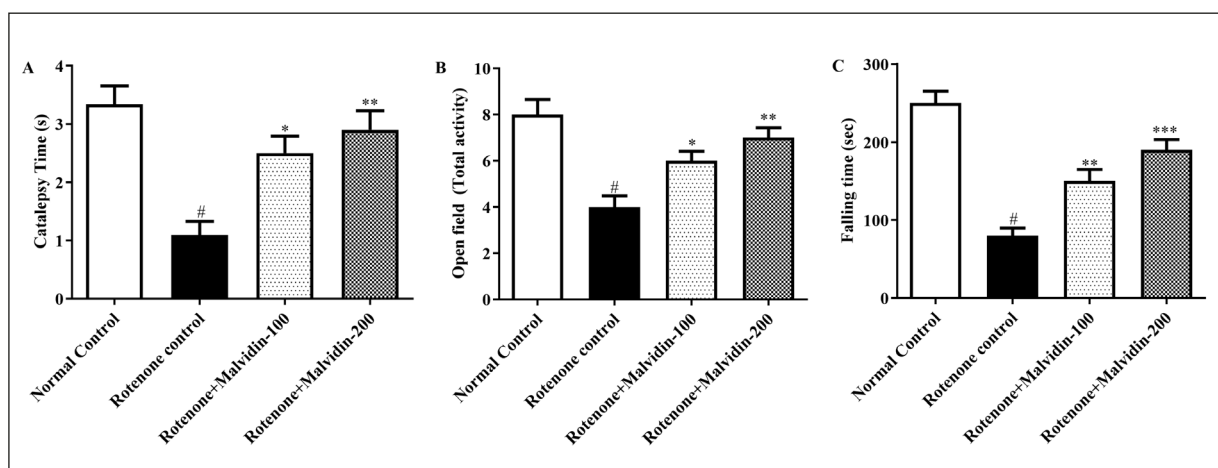


Figure 1. A-C, Effect of malvidin on behavioral parameters. **A**, Catalepsy time, **B**) Open field activity, **C**) Rotarod test. The data were expressed as mean \pm S.E.M. (n=6/group). * p <0.05, ** p <0.001, *** p <0.0001, when compared with the control group; # p <0.001 when compared with the rotenone group (one-way ANOVA followed by Tukey's test).

stricted in rotenone-treated rats collated with that in the control group. Malvidin treatment (100 and 200 mg/kg) significantly extended the retention time [F (3, 20)=28.46, p <0.0001] as associated with rotenone-induced rats (Figure 1C).

Biochemical parameters

Biochemical markers of oxidative stress, such as GSH, SOD, and CAT, showed decreased expression levels, whereas MDA levels (p <0.001) increased in the rotenone-induced animal group. The treatment groups that received both the doses of malvidin (100 and 200 mg/kg) exhibited raised levels of SOD [F (3, 20)=15.60, p <0.0001], CAT [F (3, 20)=26.36, p <0.0001], GSH [F (3, 20)=26.91, p <0.0001] and MDA [F (3, 20)=14.15, p <0.0001] expression declined as associated to rotenone control group (Figure 2A-D).

Neurotransmitters and their metabolites

The expression of DA, NE, 5-HT, DOPAC, HVA, and 5-HIAA was less (p <0.001) in the rotenone-administered subjects than that of animals in the control group. However, groups with malvidin (100 and 200 mg/kg) markedly regained the normal levels of DA [F (3, 20)=16.08, p <0.0001], NE [F (3, 20)=82.58, p <0.0001], and 5-HT [F (3, 20)=24.06, p <0.0001], DOPAC [F (3, 20)=10.66, p =0.0002], HVA [F (3, 20)=11.12, p =0.0002] and 5-HIAA [F (3, 20)=8.505, p =0.0008] as compared to rotenone control group. AChE activity was reported to be markedly decreased in rotenone-given animals com-

pared to the animals of the control group. While treatment with malvidin (100 and 200 mg/kg) was significantly restored [F (3, 20)=19.13, p <0.0001], AChE activity was associated with rotenone control. Similarly, the level of ACh was increased by rotenone in the experimental groups, while malvidin treatment significantly restored [F (3, 20)=7.111, p =0.0019] the ACh as associated with the rotenone control group (Figure 2E-L).

Neuroinflammatory markers

Rotenone administration showed a significant increase (p <0.001) in IL-1 β , IL-6, TNF- α , and caspase-3 expression in the rotenone group collated with the control group; however, Nrf-2 showed upregulation expression (p <0.001). In the malvidin-given groups (100 and 200 mg/kg) the effect of rotenone restored the expression of Nrf-2 [F (3, 20)=26.67, p <0.0001] while decreased the activity of IL-1 β [F (3, 20)=23.69], IL-6 [F (3, 20)=29.88, p <0.0001], TNF- α [F (3, 20)=13.56, p <0.0001], and caspase-3 [F (3, 20)=16.01, p <0.0001] (Figure 3A-E).

Molecular docking

We obtained the three-dimensional X-ray crystallographic structures of AChE, ChAT, TNF- α , IL-6, IL-1 β , caspase-3, and Nrf-2 from the PDB database. These structures were validated through various parameters, including resolution, mutation analysis, wwPDB validation, the presence of co-crystal ligands (Table I). Receptor grids were generated for prepared

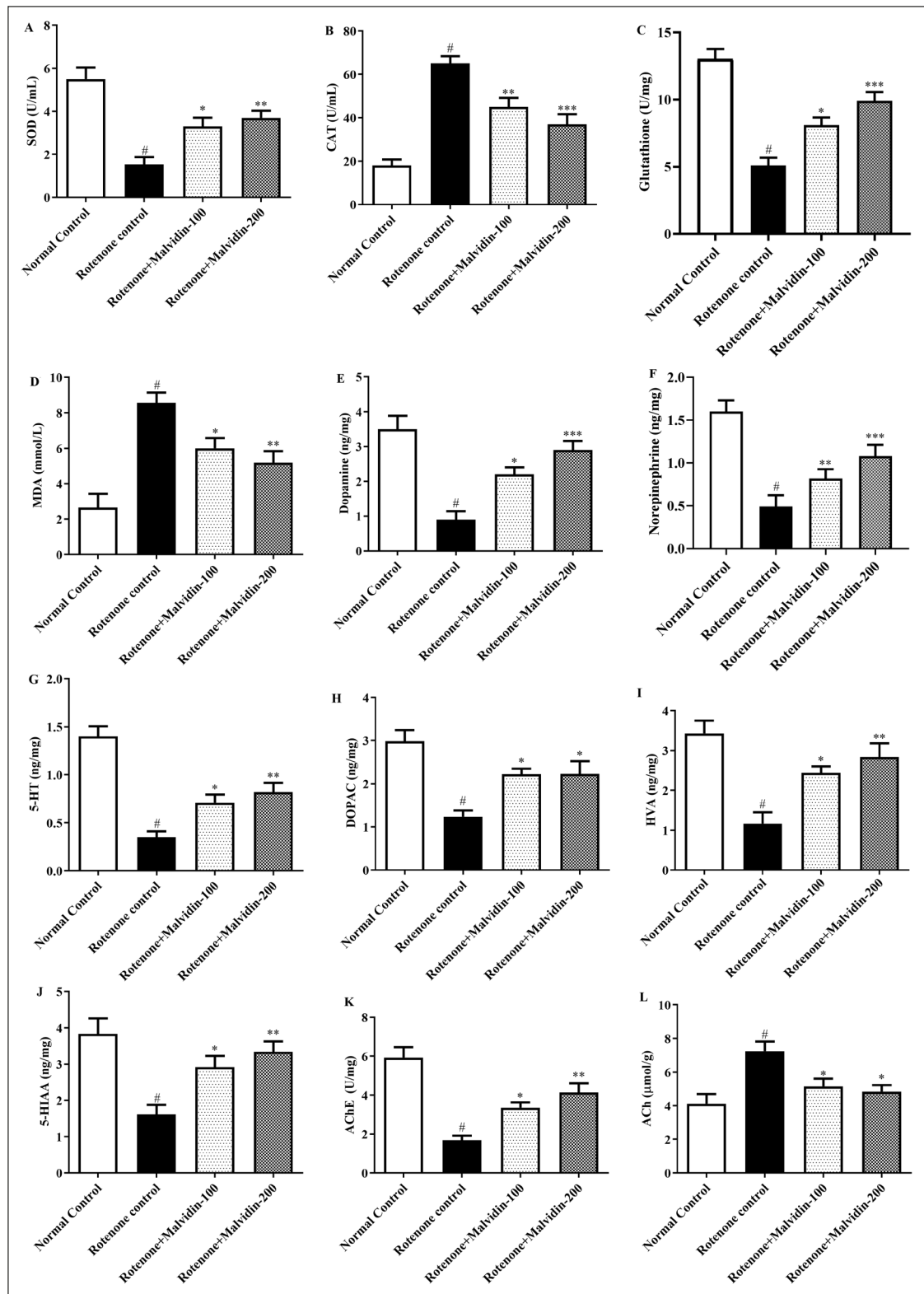


Figure 2. A-L, Effect of malvidin on antioxidant enzymes and neurotransmitters and their metabolites. **A**, Superoxide dismutase (SOD), **(B)** Catalase (CAT), **(C)** Glutathione transferase (GSH) **(D)** Malondialdehyde (MDA) **(E)** Dopamine (DA), **(F)** Norepinephrine (NE), **(G)** Serotonin (5HT), **(H)** 3,4-dihydroxyphenylacetic acid (DOPAC), **(I)** Homovanillic acid (HVA), **(J)** 5-hydroxyindoleacetic acid (5-HIAA), **(K)** Acetylcholinesterase (AChE), **(L)** Acetylcholine (ACh). The data were expressed as mean ± S.E.M. (n=6/group). **p*<0.05, ***p*<0.001, ****p*<0.0001 when compared with the control group; #*p*<0.001 when compared with rotenone group (one-way ANOVA followed by Tukey's test).

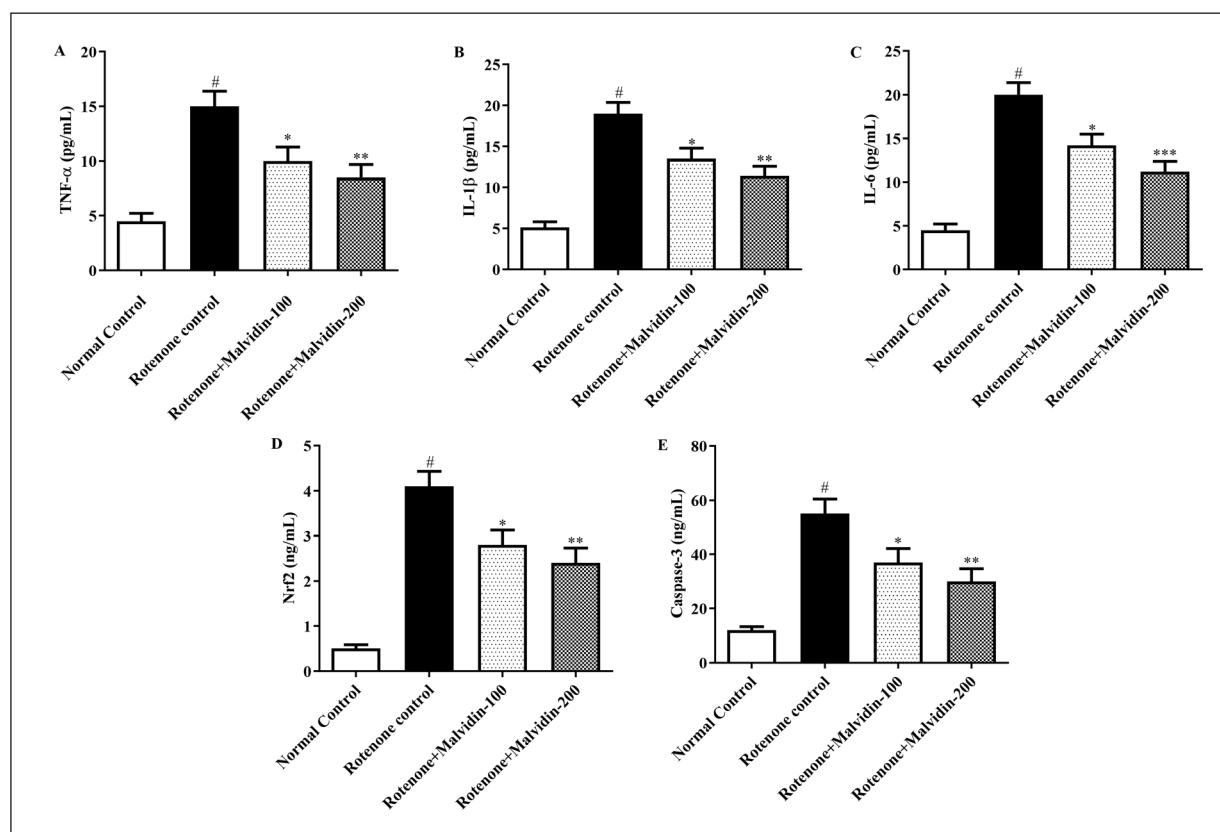


Figure 3. A-E, Effect of malvidin on neuroinflammatory parameters. **A**, Tumor necrosis factor- α (TNF- α), **(B)** interleukin-1 β (IL-1 β), **(C)** interleukin-6 (IL-6), **(D)** nuclear factor erythroid 2-related factor 2 (Nrf-2), **(E)** caspase-3. The data were expressed as mean \pm S.E.M. ($n=6$ /group). * $p<0.05$, ** $p<0.001$, *** $p<0.0001$ when compared with the control group; # $p<0.001$ when compared with rotenone group (one-way ANOVA followed by Tukey's test).

proteins (7XN1, 2FY2, 2AZ5, 1ALU, 6Y8M, 5H8Q) using AutoDockTools, Chimera, and Maestro. Grid size varied: for proteins with co-crystal ligands, dimensions were based on the ligand, while for those without, the Computed Atlas of Surface Topography of Proteins (CASTp) server determined the volume. We then analyzed amino acids lining the generated grid pockets (Table II). The enclosing box was carefully shrunk to precisely match the active site's shape and character, ensuring only compatible ligands could be docked (Table III).

The docking results indicated that AChE exhibited a favorable binding affinity towards malvidin, with a binding energy of -9.329 Kcal/mol. This interaction involves hydrophobic and hydrogen bonding with specific amino acid residues (TYR72A, ASP74A, TRP86A, GLN71A, TYR124A, SER125A, TYR337A, and TYR337A), with bond distances ranging from

2.03 to 4.00 Å. Similarly, Nrf-2 demonstrated a notable binding affinity for malvidin, yielding a binding energy of -8.253 kcal/mol. The interactions in this case included hydrophobic interactions and hydrogen bonding involving amino acid residues (SER363A, ASN382A, ARG415A, ILE416A, GLY509A, ALA510A, and SER602A) with bond distances ranging from 2.18 to 3.61 Å. Furthermore, caspase-3 exhibited a substantial affinity for malvidin, with a binding energy of -7.957 kcal/mol. This interaction is characterized by a combination of hydrophobic interactions and hydrogen bonding, with bond distances ranging from 2.18 to 3.61 Å. The amino acid residues involved were SER363A, ASN382A, ARG415A, ARG415A, ILE416A, GLY509A, ALA510A, and SER602A. In contrast, IL-6 demonstrated the lowest affinity for malvidin, with a binding energy of -5.956 kcal/mol. The findings are summarized in (Table IV

Table I. A comparison of standard values and retrieved proteins for validation of protein selection in docking studies.

Parameters	Protein details						Standards
Targets	Acetylcholinesterase	Tumor necrosis factor- α	Interleukin-6	Interleukin-1 β	Caspase-3	Nuclear factor erythroid 2-related factor 2	
Protein Id	7XN1	2AZ5	1ALU	6Y8M	1NME	5FZN	-
Method of experiment	X-ray diffraction	X-ray diffraction	X-ray diffraction	X-ray diffraction	X-ray diffraction	X-ray diffraction	X-ray diffraction
Mutation	No	No	No	No	No	No	No
Resolution	2.85 Å	2.10 Å	1.90 Å	1.90 Å	1.60 Å	1.97 Å	Near about 2.00 Å
wwPDB Validation	Better	Better	Better	Better	Better	Better	Better
Co-Crystal Ligand	THA	307	Absent	SX2	159	FB2	-
Ramchandran Plot (by PROCHECK server)							
Residues in favored + Allowed regions	89.8%	90.2%	90%	89%	90.2	90.0%	>80%

Table II. Active sites amino acids.

Protein	Active sites amino acids
7XN1	ASP74, TRP86, GLY121, GLU202, TYR337, TYR341, HIS447, GLY448
2FY2	TYR28, CYS31, MET32, TRP80, ASP83, MET84, TYR85, ASN88, LEU90, LEU92, VAL94, ASN95, SER96, SER97, PRO98, VAL100, ILE136, PRO137, THR138, GLY147, GLN148, LEU150, MET152, GLN154, TYR155, ARG163, ARG240, CYS322, HIS324, PHE327, ASP328, GLY329, ILE330, VAL331, LEU332, VAL333, GLN334, GLU337, LYS403, LYS407, CYS411, SER412, PRO413, ASP414, ALA415, TYR436, GLU437, SER438, ALA439, SER440, ARG442, ARG443, ARG448, VAL449, ASP450, ASN451, ILE452, ARG453, GLN489, THR490, THR493, VAL494, ILE497, ILE502, ASP503, ASN504, LEU506, LEU507, ARG510, TYR529, SER532, ASN533, PHE535, SER538, THR539, SER540, GLN541, VAL542, PRO543, THR544, THR545, CYS550, TYR552, GLY553, PRO554, VAL555, VAL556, PRO557, PRO566, GLN567, PHE578
2AZ5	LEU57A, TYR59A, SER60A, TYR119A, LEU120A, GLY121A, GLY122A, TYR151A, LEU57B, TYR59B, SER60B, TYR119B, LEU120B, GLY121B, TYR151B, LEU55D
1ALU	GLU95, VAL96, LEU98, GLU99, GLN116, LYS120, PRO141, ASN144
6Y8M	GLU105A, ASN108A, LYS109A, LEU110A, THR147A, MET148A, GLN149A
5H8Q	PHE18, ILE116, SER121, VAL124, ASP125, PHE126, VAL128, PRO129, PHE130, VAL131, GLU132, ILE135, ARG141, THR146, GLY147, LEU148, SER149, ASN176, ASN180, TYR181, ALA215, ALA216, ASN219, TYR220, ALA222, GLY223, ARG224, CYS228, LEU230, VAL231, THR232, GLY234, SER235, GLY236, TYR237, ILE238, PHE239, ALA240, THR241, THR242, GLY243, LYS250, LYS255, ARG256, ASP259, LEU260, LEU262, LEU263, GLN264, VAL266, GLY267, ASP268, GLY269, MET271, GLU272, GLU275, THR276, LEU279, THR280, GLY281, CYS283, PHE67, THR127, ILE128, ASN129, ASN130, GLU131, ALA133, GLN134, ILE136, GLU137, PHE138, SER139, LYS140, PRO141, PHE142, LYS143, TYR144, GLN145, LEU147, ILE160, ARG166, SER181, VAL182, ILE184, TYR185, ARG188, GLN189, GLU191, LEU192, ASP225, SER226, ALA227, GLU230, PHE231, GLU244, LEU245, PHE246, PHE247, ARG248, SER249, GLY250, MET255, LYS257, LYS262, GLN263, SER266, LEU267, LEU270, HIS273, GLU274, ASN275, GLY276, MET278, GLU279, ASP282, LYS283, VAL286, ARG287
1NME	TRP206, ARG207, ASN208, SER209, LYS210, TRP214, SER249, PHE250, SER251, PHE252
5FZN	TYR334A, TYR334A, SER363A, SER363A, GLY364A, GLY364A, ARG415A, ARG415A, ARG415A, ARG415A, ARG415A, ALA556A, ALA556A, SER602A, SER602A, SER602A, GLY603A, GLY603A, GLY603A

and Figure 4).

Discussion

In the present work, the neuroprotective properties of malvidin were analyzed in rotenone-administered experimental rats. Based on behavioral test findings, rotenone administration

markedly affected locomotor activity and motor coordination in experimental animals. Moreover, neurotransmitter analysis revealed dopaminergic neurodegeneration in the striata of rotenone-treated rodents. These observations were in line with those of a previous investigation³⁴. Previous research³⁵⁻³⁷ has shown that rotenone administra-

Table III. Grid parameter.

PDB ID	Centre coordinates			Size coordinates		
	X	Y	Z	X	Y	Z
7XN1	48.32	-40.0	-30.0	40	40	40
2FY2	9.603	0.134	66.752	40	40	40
2AZ5	-19.41	-74.65	33.85	35	35	35
1ALU	9.966	-20.835	16.696	30	30	30
6Y8M	7.3	25.32	-9.44	40	40	40
5H8Q	14.66	-14.25	-25.73	20	20	20
1NME	42.09	96.34	24.13	30	30	30
5FZN	14.02	66.12	30.64	20	20	20

tion in experimental animals produces symptoms that mimic Parkinson's disease, including oxidative damage, neuroinflammation, apoptosis, and behavioral and biochemical changes. Rotenone induction causes microglia-mediated neuronal inflammation, which results in blood-brain barrier dysfunction and damage to dopaminergic neurons³⁸. Previous work^{4,39,40} showed that rotenone treatment in animals results in cognitive imbalances, impairment in coordination, gait dysfunction, and paralysis supported by behavioral tests such as catalepsy, rotarod, and open-field tests. In previous studies^{41,42}, malvidin significantly improved the behavioral parameters in experimental animals, including rota-rod test, open field test, and catalepsy test. Similarly, in the present exper-

iments, malvidin treatment (100 and 200 mg/kg) reversed the effects of rotenone in animals and normalized the learning ability.

Malvidin was reported to have antioxidant properties inhibiting oxidative stress and ameliorating the chemically induced neurodegenerative effects in animal models⁴². Previous research^{6,20} has shown that oxidative stress causes damage to dopaminergic neurons in the brain tissue. The current observations are supported by previous research^{36,43} that demonstrated that rotenone administration caused neurodegenerative damage *via* oxidative stress by lowering the expression of SOD, GSH, and CAT and promoting MDA activity. The current study demonstrated that malvidin mitigated rotenone-induced oxidative

Table IV. Docking Score and intermolecular interactions of ligands Malvidin Proteins acetylcholinesterase (7XN1), choline acetyltransferase (2FY2), tumor necrosis factor- α (2AZ5), interleukin-6 (1ALU), interleukin-1 β (6Y8M), glutamate (5H8Q) caspase-3 (1NME), NRF-2(5FZN) using LigPlot v1.4.5, PLIP server, Maestro V12.8 and Biovia Discovery studio visualizer.

Sr. No.	Proteins	Binding Energy Kcal/mol	Interactions	Residue ID	Distance
1	7XN1_Malvidin	-9.329	Hydrophobic Interactions Hydrogen Bonds p-Stacking	TYR72A ASP74A TRP86A GLN71A TYR124A SER125A TYR337A TYR337A HIS447A TRP86A TRP86A TYR124A	3.87 3.75 4 2.43 3.01 3.32 2.03 2.3 2.18 3.85 3.95 5.26
2	2FY2_Malvidin	-8.234	Hydrophobic Interactions Hydrogen Bonds	VAL542A HIS324A GLY329A ILE330A GLN541A	3.81 2.15 2.43 3.01 3.1
3	2AZ5_Malvidin	-6.632	Hydrogen Bonds p-Stacking	TYR119A GLY121A TYR151A TYR119A TYR119A	2.54 2.16 2.48 4.04 4.17
4	1ALU_Malvidin	-5.956	Hydrophobic Interactions Hydrogen Bonds	GLU93A PRO139A ASP140A THR143A GLU93A ASP140A THR143A	3.56 3.64 3.9 3.89 2.2 2.55 2.2
5	6Y8M_MALVIDIN	-6.809	Hydrogen Bonds	SER5A SER5A SER43A SER43A LYS65A TYR68A	2.26 3.35 3.07 3.14 1.97 2.54

Continued

Table IV (Continued). Docking Score and intermolecular interactions of ligands Malvidin Proteins acetylcholinesterase (7XN1), choline acetyltransferase (2FY2), tumor necrosis factor- α (2AZ5), interleukin-6 (1ALU), interleukin-1 β (6Y8M), glutamate (5H8Q) caspase-3 (1NME), NRF-2(5FZN) using LigPlot v1.4.5, PLIP server, Maestro V12.8 and Biovia Discovery studio visualizer.

Sr. No.	Proteins	Binding Energy Kcal/mol	Interactions	Residue ID	Distance
6	5H8Q_MALVIDIN	-9.754	Hydrophobic Interactions	PRO129A	3.3
				PRO141B	3.59
				TYR144B	3.38
			Hydrogen Bonds	GLU132A	2.72
				PRO141B	3.16
				TYR144B	3.56
				TYR144B	3.33
				THR241A	2.64
				THR242A	3.32
			p-Stacking	GLY250B	2.34
TYR144B	3.98				
7	1NME_MALVIDIN	-7.957	Hydrophobic Interactions	ARG415A	3.48
				ALA556A	3.13
			Hydrogen Bonds	SER363A	2.19
				ASN382A	3.02
				ARG415A	2.28
				ARG415A	2.84
				ILE416A	2.66
				GLY509A	3.61
				ALA510A	3.23
				SER602A	2.18
8	5FZN_MALVIDIN	-8.253	Hydrophobic Interactions	ARG415A	3.48
				ALA556A	3.13
			Hydrogen Bonds	SER363A	2.19
				ASN382A	3.02
				ARG415A	2.28
				ARG415A	2.84
				ILE416A	2.66
				GLY509A	3.61
				ALA510A	3.23
				SER602A	2.18

stress in rodents at doses of 100 and 200 mg/kg. ROS generation due to oxidative stress, accompanied by neuroinflammation, results in the progression of neurodegenerative disorders. CAT are defense mechanisms that neutralize free radicals by converting H_2O_2 into water and oxygen molecules.

Similarly, SOD produces superoxide anions that neutralize oxidative stress⁴². In this study, treatment with both concentrations of malvidin (200 and 100 mg/kg) markedly raised CAT and SOD levels, resulting in a decline in oxidative stress. GSH is a prominent scavenger of ROS, which suppresses oxidative injury and is used as a marker of oxidative stress. Previous findings⁴⁴, which are in agreement with the current results, have revealed an increase in GSH activity in experimental animals treated with malvidin. MDA is an output of lipid peroxidation, and its

elevated levels indicate an increase in the level of oxidative stress. Previous studies⁴⁵ have revealed elevated MDA levels in neurodegenerative disorders, which is in line with current work. The output of the present work showed that malvidin treatment markedly reduced MDA expression in experimental animals. Malvidin may reduce the risk of neurodegenerative diseases and protect the brain from oxidative damage.

A previous study⁴⁶ reported that 5-HT and NE are crucial in normal psychological behavior and that dopamine plays a crucial role in movement. In the present results, rotenone administration lowered DA, NE, 5-HIAA, and 5-HT levels but increased HVA and DOPAC expression, analogous to earlier findings^{47,48}. Treatment with malvidin restored the effects of rotenone in experimental animals, resulting in normal levels of neurotransmitters, which improved the neuronal

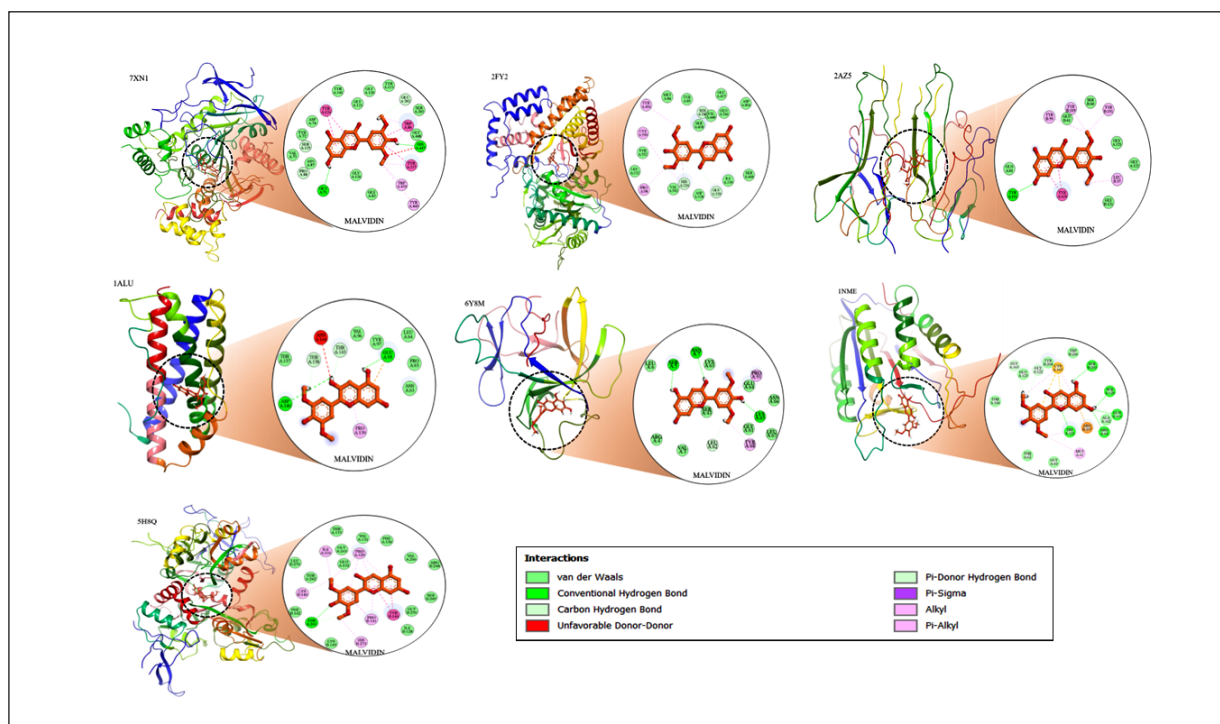


Figure 4. A-G, Molecular docking of the Malvidin with (A) acetylcholinesterase (AChE) (7XN1), (B) Choline acetyltransferase (ChAT) (2FY2), (C) Tumor necrosis factor- α (TNF- α) (2AZ5), (D) interleukin-6 (IL-6) (1ALU), (E) interleukin-1 β (IL-1 β) (6Y8M), (F) caspase-3 (1NME), and (G) nuclear factor erythroid 2-related factor 2 (NRF-2) (5FZN) Proteins.

and behavioral activities of rodents. As a result, malvidin might be beneficial for maintaining brain levels of dopamine and serotonin.

AChE plays a prominent role in the hydrolysis of the neurotransmitter ACh, which is necessary for the normal functioning of memory, locomotion, and the learning ability of an individual. A disturbance between dopamine and ACh in the striatum results in the progression of PD^{49,50}. Previous animal studies⁴² have shown that rotenone administration increases AChE activity, which agrees with the outputs of the present work. Earlier literature has depicted that malvidin improves cognitive ability by reducing AChE activity, which supports our findings that treatment with malvidin significantly inhibits AChE activity. Moreover, it was previously demonstrated that malvidin improves cognitive ability by reducing AChE activity, which supports our findings that treatment with malvidin significantly inhibits AChE activity. A previous study⁵¹ suggests that an abnormal increase in the ACh level causes cholinergic activity and dopaminergic inhibition, resulting in dopaminergic and cholinergic imbalances. Previous research⁵² demonstrated that rotenone increases ACh levels, which is consistent with our observations. In the

present study, malvidin significantly normalized ACh levels in experimental animals. Malvidin increases acetylcholine levels in the brain by inhibiting AChE, the enzyme responsible for breaking down ACh. As a result, cognitive function and memory can be improved.

The neurodegeneration is associated with neuronal inflammation caused by alterations in inflammatory cytokine expression⁵³. Previous findings⁵⁴ have shown that rotenone administrations in animals result in the release of inflammatory molecules such as TNF- α , IL-1 β , and IL-6 by activated astrocytes and microglia. Malvidin reverses chemically induced inflammation by depleting proinflammatory cytokine levels, as shown in the literature. Moreover, in a previous investigation⁵⁵, malvidin was reported to suppress the transcription of genes encoding proinflammatory cytokines. These molecular mechanisms may be responsible for the anti-inflammatory activity of malvidin in reversing the neurodegenerative effects in rodents. Another study⁵⁶ revealed the anti-inflammatory activity of malvidin, in which malvidin downregulated the gene expression of molecules that trigger inflammation, which may participate in suppressing neuroinflammation

in malvidin-treated rats. The current results revealed that experimental animals treated with malvidin showed significant decreases in IL-6, IL-1 β , and TNF- α expressions. As a result of malvidin's ability to reduce neuroinflammation, the brain may be protected from damage.

Nrf-2 antioxidant signaling inhibits the expression of TNF- α and other proinflammatory cytokines by attenuating inflammatory responses⁵⁷. A recent study⁵⁸ found that exposure to rotenone significantly inhibits the expression of the Nrf-2 pathway in the striatum. Fan et al⁵⁹ described that malvidin regulates Nrf-2 signaling, suppresses oxidative stress, and decreases inflammatory effects by inhibiting proinflammatory cytokines. In the present study, rotenone suppressed the activity of Nrf-2 in rotenone-treated rodents compared to the control group. Supporting the findings of the current investigation, Xu et al⁴⁴ revealed that malvidin activates the Nrf-2 signaling pathway in the malvidin treatment group. Malvidin may contribute to brain protection and inflammation reduction by reducing oxidative damage. According to the results of a previous study⁶⁰, rotenone damages dopaminergic neurons *via* caspase-3-triggered apoptosis. In the present study, caspase-3 activity was promoted in the rotenone group than in the control group. According to the study of Sari et al⁶¹, anthocyanin (malvidin) is a potent inhibitor of caspase-3 signaling and, thus, possesses anti-apoptotic activity. Our results show that malvidin reduced the rotenone-induced activity of caspase-3 in rats, which may be the mechanism responsible for the protective effects of malvidin. Malvidin may help to protect brain cells from damage and reduce the risk of neurodegenerative diseases.

Our molecular docking results are consistent with those of prior literature; the binding free energy serves as a crucial parameter for assessing the strength of a drug's interaction with a protein. A low (negative) binding energy indicates favorable binding between the drug and target molecule, whereas a high (positive) binding energy signifies weak or unfavorable interactions between the drug and target protein^{62,63}. Previous studies^{64,65} of neurodegenerative disorders demonstrated that AChE exhibits substantial affinity for potential drug molecules with low binding energy scores and thus can serve as a potential drug target. Similarly, our findings revealed a high binding affinity between malvidin and AChE with low binding energy. Additionally, it is noteworthy that malvidin exhibited a strong

binding affinity for Nrf-2 and caspase-3, resulting in low binding energies. These observations indicate that malvidin holds promise as a potential therapeutic agent that specifically targets AChE, caspase-3, and Nrf-2. These proteins are key targets for further investigation, particularly in the context of rotenone-induced PD.

Overall, the present study has few limitations in explaining the neuroprotective mechanism of malvidin at the molecular level. Thus, gene and protein expression studies will be required on genes and proteins that have crucial roles in neuroprotective mechanisms, such as the antioxidant, anti-inflammatory, and antiapoptotic pathways. Further, to confirm the mechanism or effect of malvidin, further studies with different paradigms are essential.

Conclusions

The study revealed that malvidin has neuroprotective properties against the rotenone induced PD. Malvidin effectively restored the behavioral deficits and normalized the oxidative stress and neuroinflammation induced by Rotenone. Hence, malvidin could be considered a potential therapeutic candidate against PD. Both (200 and 100 mg/kg) doses of malvidin effectively reversed the alternations caused by rotenone; however, a high dose (200 mg/kg) was reported to have more profound effects. However, further studies should be carried out to explore the molecular mechanism behind the neuroprotective properties of malvidin.

Ethics Approval

The work was approved by the Institutional Animal Ethics Committee of T. G. Lab, India (IAEC/TRS/PT/23/29).

Informed Consent

Not applicable due to the design of the study.

Funding

This research work was funded by the Deanship Scientific of Research (DSR) at King Abdulaziz University, Jeddah, Saudi Arabia, with grant No. G: 580-130-1441.

Acknowledgments

This project was funded by the Deanship of Research (DSR), King Abdulaziz University, Jeddah, under grant No. G: 580-130-1441. The authors, therefore, acknowledge with thanks DSR for technical and financial support.

Authors' Contributions

IK designed and performed experimental work and analyzed data; MSN and MA drafted the manuscript. FAA, NARA, RAS, SDA, and FA critically revised the manuscript.

Conflicts of Interest

The authors have no competing interests to declare.

Data Availability

All data generated or analyzed during this study are included in this article. Further inquiries can be directed to the corresponding author.

ORCID ID

Imran Kazmi: 0000-0003-1881-5219
 Fahad A. Al-Abbasi: 0000-0001-5609-4913
 Naif A. R. Almalki: 0000-0002-1142-607X
 Ryan A. Sheikh: 0000-0003-3275-0861
 Salwa D. Al-Qahtani: 0009-0007-2223-3031
 Muhammad Shahid Nadeem: 0000-0003-4112-0925
 Sarwar Beg: 0000-0002-3304-2712
 Muhammad Afzal: 0000-0003-0517-4934

References

- Sharma S, Kumar P, Deshmukh R. Neuroprotective potential of spermidine against rotenone induced Parkinson's disease in rats. *Neurochem Int* 2018; 116: 104-111.
- Zhang X, Du L, Zhang W, Yang Y, Zhou Q, Du G. Therapeutic effects of baicalein on rotenone-induced Parkinson's disease through protecting mitochondrial function and biogenesis. *Sci Rep* 2017; 7: 1-14.
- Michel HE, Tadros MG, Esmat A, Khalifa AE, Abdel-Tawab AM. Tetramethylpyrazine ameliorates rotenone-induced Parkinson's disease in rats: involvement of its anti-inflammatory and anti-apoptotic actions. *Mol Neurobiol* 2017; 54: 4866-4878.
- Khatri DK, Juvekar AR. Neuroprotective effect of curcumin as evinced by abrogation of rotenone-induced motor deficits, oxidative and mitochondrial dysfunctions in mouse model of Parkinson's disease. *Pharmacol Biochem Behav* 2016; 150: 39-47.
- Alzahrani S, Ezzat W, Elshaer R, Abd El-Lateef A, Mohammad H, Elkazaz A, Toraih E, Zaitone S. Standardized Tribulus terrestris extract protects against rotenone-induced oxidative damage and nigral dopamine neuronal loss in mice. *J Physiol Pharmacol* 2018; 69: 979-994.
- Anusha C, Sumathi T, Joseph LD. Protective role of apigenin on rotenone induced rat model of Parkinson's disease: Suppression of neuroinflammation and oxidative stress mediated apoptosis. *Chem Biol Interact* 2017; 269: 67-79.
- Palle S, Neerati P. Improved neuroprotective effect of resveratrol nanoparticles as evinced by abrogation of rotenone-induced behavioral deficits and oxidative and mitochondrial dysfunctions in rat model of Parkinson's disease. *Naunyn Schmiedebergs Arch Pharmacol* 2018; 391: 445-453.
- Darbinyan L, Hambardzumyan L, Simonyan K, Chavushyan V, Manukyan L, Badalyan S, Khalaji N, Sarkisian V. Protective effects of curcumin against rotenone-induced rat model of Parkinson's disease: In vivo electrophysiological and behavioral study. *Metab Brain Dis* 2017; 32: 1791-1803.
- Medeiros-Linard CFB, Andrade-da-Costa BLdS, Augusto RL, Sereniki A, Trevisan MTS, Perreira RdCR, de Souza FTC, Braz GRF, Lagranha CJ, de Souza IA. Anacardic acids from cashew nuts prevent behavioral changes and oxidative stress induced by rotenone in a rat model of Parkinson's disease. *Neurotox Res* 2018; 34: 250-262.
- Zhang L, Hao J, Zheng Y, Su R, Liao Y, Gong X, Liu L, Wang X. Fucoidan protects dopaminergic neurons by enhancing the mitochondrial function in a rotenone-induced rat model of Parkinson's disease. *Aging Dis* 2018; 9: 590.
- Zhang N, Dou D, Ran X, Kang T. Neuroprotective effect of arctigenin against neuroinflammation and oxidative stress induced by rotenone. *RSC Adv* 2018; 8: 2280-2292.
- Zhang Z, Sun X, Wang K, Yu Y, Zhang L, Zhang K, Gu J, Yuan X, Song G. Hydrogen-saturated saline mediated neuroprotection through autophagy via PI3K/AKT/mTOR pathway in early and medium stages of rotenone-induced Parkinson's disease rats. *Brain Res Bull* 2021; 172: 1-13.
- Khoo HE, Azlan A, Tang ST, Lim SM. Anthocyanidins and anthocyanins: colored pigments as food, pharmaceutical ingredients, and the potential health benefits. *Food Nutr Res* 2017; 61: 1361779.
- Petruk G, Illiano A, Del Giudice R, Raiola A, Amoresano A, Rigano MM, Piccoli R, Monti DM. Malvidin and cyanidin derivatives from açai fruit (*Euterpe oleracea* Mart.) counteract UV-A-induced oxidative stress in immortalized fibroblasts. *J Photochem Photobiol B* 2017; 172: 42-51.
- Baba AB, Nivetha R, Chattopadhyay I, Nagini S. Blueberry and malvidin inhibit cell cycle progression and induce mitochondrial-mediated apoptosis by abrogating the JAK/STAT-3 signalling pathway. *Food Chem Toxicol* 2017; 109: 534-543.
- Li D, Wang P, Luo Y, Zhao M, Chen F. Health benefits of anthocyanins and molecular mechanisms: Update from recent decade. *Crit Rev Food Sci Nutr* 2017; 57: 1729-1741.

- 17) Hair R, Sakaki JR, Chun OK. Anthocyanins, Microbiome and Health Benefits in Aging. *Molecules* 2021; 26: 537.
- 18) Sidorova YA, Volcho KP, Salakhutdinov NF. Neuroregeneration in Parkinson's Disease: From Proteins to Small Molecules. *Curr Neuropharmacol* 2019; 17: 268-287.
- 19) Carrera I, Cacabelos R. Current drugs and potential future neuroprotective compounds for Parkinson's disease. *Curr Neuropharmacol* 2019; 17: 295-306.
- 20) Javed H, Meeran MN, Azimullah S, Bader Eddin L, Dwivedi VD, Jha NK, Ojha S. α -Bisabolol, a dietary bioactive phytochemical attenuates dopaminergic neurodegeneration through modulation of oxidative stress, neuroinflammation and apoptosis in rotenone-induced rat model of Parkinson's disease. *Biomolecules* 2020; 10: 1421.
- 21) Ali DE, Bassam SM, Elatrebi S, Habiba ES, Allam EA, Omar EM, Ghareeb DA, Abdulmalek SA, Abdel-Sattar E. HR LC-MS/MS metabolomic profiling of *Yucca aloifolia* fruit and the potential neuroprotective effect on rotenone-induced Parkinson's disease in rats. *PloS One* 2023; 18: e0282246.
- 22) Percie du Sert N, Hurst V, Ahluwalia A, Alam S, Avey MT, Baker M, Browne WJ, Clark A, Cuthill IC, Dirnagl U. The ARRIVE guidelines 2.0: Updated guidelines for reporting animal research. *J Cereb Blood Flow Metab* 2020; 40: 1769-1777.
- 23) Badawi GA, Abd El Fattah MA, Zaki HF, El Sayed MI. Sitagliptin and liraglutide reversed nigrostriatal degeneration of rodent brain in rotenone-induced Parkinson's disease. *Inflammopharmacology* 2017; 25: 369-382.
- 24) Altharawi A, Alharthy KM, Altharwi HN, Albaqami FF, Alzarea SI, Al-Abbasi FA, Nadeem MS, Kazmi I. Europinidin Inhibits Rotenone-Activated Parkinson's Disease in Rodents by Decreasing Lipid Peroxidation and Inflammatory Cytokines Pathways. *Molecules* 2022; 27.
- 25) Shin MS, Kim TW, Lee JM, Ji ES, Lim BV. Treadmill exercise alleviates nigrostriatal dopaminergic loss of neurons and fibers in rotenone-induced Parkinson rats. *J Exerc Rehabil* 2017; 13: 30-35.
- 26) Ramkumar M, Rajasankar S, Gobi VV, Janakiraman U, Manivasagam T, Thenmozhi AJ, Essa MM, Chidambaram R, Chidambaram SB, Guillemain GJ. Demethoxycurcumin, a Natural Derivative of Curcumin Abrogates Rotenone-induced Dopamine Depletion and Motor Deficits by Its Antioxidative and Anti-inflammatory Properties in Parkinsonian Rats. *Pharmacogn Mag* 2018; 14: 9-16.
- 27) Góth L. A simple method for determination of serum catalase activity and revision of reference range. *Clin Chim Acta* 1991; 196: 143-151.
- 28) Sharma N, Bafna P. Effect of *Cynodon dactylon* on rotenone induced Parkinson's disease. *Orient Pharm Exp Med* 2012; 12: 167-175.
- 29) Tseng HC, Wang MH, Chang KC, Soung HS, Fang CH, Lin YW, Li KY, Yang CC, Tsai CC. Protective Effect of (-)Epigallocatechin-3-gallate on Rotenone-Induced Parkinsonism-like Symptoms in Rats. *Neurotox Res* 2020; 37: 669-682.
- 30) Abdel-Salam OME, Youness ER, Ahmed NA, El-Toumy SA, Souleman AMA, Shaffie N, Abouelfadl DM. *Bougainvillea spectabilis* flowers extract protects against the rotenone-induced toxicity. *Asian Pac J Trop Med* 2017; 10: 478-490.
- 31) Sedaghat R, Roghani M, Khalili M. Neuroprotective effect of thymoquinone, the *nigella sativa* bioactive compound, in 6-hydroxydopamine-induced hemi-parkinsonian rat model. *Iran J Pharm Res* 2014; 13: 227-234.
- 32) Batool Z, Sadir S, Liaquat L, Tabassum S, Madiha S, Rafiq S, Tariq S, Batool TS, Saleem S, Naqvi F, Perveen T, Haider S. Repeated administration of almonds increases brain acetylcholine levels and enhances memory function in healthy rats while attenuates memory deficits in animal model of amnesia. *Brain Res Bull* 2016; 120: 63-74.
- 33) Haider S, Saleem S, Perveen T, Tabassum S, Batool Z, Sadir S, Liaquat L, Madiha S. Age-related learning and memory deficits in rats: role of altered brain neurotransmitters, acetylcholinesterase activity and changes in antioxidant defense system. *Age (Dordr)* 2014; 36: 9653.
- 34) El-Shamarka MEA, Kozman MR, Messiha BAS. The protective effect of inosine against rotenone-induced Parkinson's disease in mice; role of oxido-nitrosative stress, ERK phosphorylation, and A2AR expression. *Naunyn Schmiedebergs Arch Pharmacol* 2020; 393: 1041-1053.
- 35) Zhang Y, Guo H, Guo X, Ge D, Shi Y, Lu X, Lu J, Chen J, Ding F, Zhang Q. Involvement of Akt/mTOR in the neurotoxicity of rotenone-induced Parkinson's disease models. *Int J Environ Res Public Health* 2019; 16: 3811.
- 36) Verma R, Nehru B. Effect of centrophenoxine against rotenone-induced oxidative stress in an animal model of Parkinson's disease. *Neurochem Int* 2009; 55: 369-375.
- 37) Zhang D, Li S, Hou L, Jing L, Ruan Z, Peng B, Zhang X, Hong J-S, Zhao J, Wang Q. Microglial activation contributes to cognitive impairments in rotenone-induced mouse Parkinson's disease model. *J Neuroinflammation* 2021; 18: 1-16.
- 38) Ruan Z, Zhang D, Huang R, Sun W, Hou L, Zhao J, Wang Q. Microglial Activation Damages Dopaminergic Neurons through MMP-2/-9-Mediated Increase of Blood-Brain Barrier Permeability in a Parkinson's Disease Mouse Model. *Int J Mol Sci* 2022; 23: 2793.
- 39) Zaitone SA, Ahmed E, Elsherbiny NM, Mehanana ET, El-Kherbetawy MK, ElSayed MH, Alsharief DM, Moustafa YM. Caffeic acid improves locomotor activity and lessens inflammatory

- burden in a mouse model of rotenone-induced nigral neurodegeneration: Relevance to Parkinson's disease therapy. *Pharmacol Rep* 2019; 71: 32-41.
- 40) Huang J, Liu H, Gu W, Yan Z, Xu Z, Yang Y, Zhu X, Li Y. A delivery strategy for rotenone microspheres in an animal model of Parkinson's disease. *Biomaterials* 2006; 27: 937-946.
 - 41) D'Amico R, Impellizzeri D, Genovese T, Fusco R, Peritore AF, Crupi R, Interdonato L, Franco G, Marino Y, Arangia A. Açai berry mitigates Parkinson's disease progression showing dopaminergic neuroprotection via Nrf2-HO1 pathways. *Mol Neurobiol* 2022; 59: 6519-6533.
 - 42) Gilani SJ, Bin-Jumah MN, Al-Abbasi FA, Imam SS, Alshehri S, Ghoneim MM, Shahid Nadeem M, Afzal M, Alzarea SI, Sayyed N. Antiamnesic Potential of Malvidin on Aluminum Chloride Activated by the Free Radical Scavenging Property. *ACS Omega* 2022; 7: 24231-24240.
 - 43) Saravanan KS, Sindhu KM, Mohanakumar KP. Melatonin protects against rotenone-induced oxidative stress in a hemiparkinsonian rat model. *J Pineal Res* 2007; 42: 247-253.
 - 44) Xu Y, Ke H, Li Y, Xie L, Su H, Xie J, Mo J, Chen W. Malvidin-3-O-Glucoside from blueberry ameliorates nonalcoholic fatty liver disease by regulating transcription factor EB-mediated lysosomal function and activating the Nrf2/ARE signaling pathway. *J Agric Food Chem* 2021; 69: 4663-4673.
 - 45) Liu X, Zheng F, Li S, Wang Z, Wang X, Wen L, He Y. Malvidin and its derivatives exhibit antioxidant properties by inhibiting MAPK signaling pathways to reduce endoplasmic reticulum stress in ARPE-19 cells. *Food Funct* 2021; 12: 7198-7213.
 - 46) Blows WT. Neurotransmitters of the brain: serotonin, noradrenaline (norepinephrine), and dopamine. *J Neurosci Nurs* 2000; 32: 234-238.
 - 47) Sharma S, Raj K, Singh S. Neuroprotective effect of quercetin in combination with piperine against rotenone-and iron supplement-induced Parkinson's disease in experimental rats. *Neurotox Res* 2020; 37: 198-209.
 - 48) Dodiya HB, Forsyth CB, Voigt RM, Engen PA, Patel J, Shaikh M, Green SJ, Naqib A, Roy A, Kordower JH. Chronic stress-induced gut dysfunction exacerbates Parkinson's disease phenotype and pathology in a rotenone-induced mouse model of Parkinson's disease. *Neurobiol Dis* 2020; 135: 104352.
 - 49) Pervin M, Hasnat MA, Lee YM, Kim DH, Jo JE, Lim BO. Antioxidant Activity and Acetylcholinesterase Inhibition of Grape Skin Anthocyanin (GSA). *Molecules* 2014; 19: 9403-9418.
 - 50) Huang Q, Liao C, Ge F, Ao J, Liu T. Acetylcholine bidirectionally regulates learning and memory. *J Neurorestoratol* 2022; 10: 100002.
 - 51) Swathi G, Bhuvaneshwar C, Rajendra W. Alterations of cholinergic neurotransmission in rotenone induced parkinson's disease: protective role of bacopa monnieri. *Int J Pharm Biol Sci* 2013; 3: 286-292.
 - 52) Ablat N, Lv D, Ren R, Xiaokaiti Y, Ma X, Zhao X, Sun Y, Lei H, Xu J, Ma Y, Qi X, Ye M, Xu F, Han H, Pu X. Neuroprotective Effects of a Standardized Flavonoid Extract from Safflower against a Rotenone-Induced Rat Model of Parkinson's Disease. *Molecules* 2016; 21: 1107.
 - 53) Singh B, Pandey S, Rumman M, Mahdi AA. Neuroprotective effects of Bacopa monnieri in Parkinson's disease model. *Metab Brain Dis* 2020; 35: 517-525.
 - 54) Jayaraj RL, Azimullah S, Parekh KA, Ojha SK, Beiram R. Effect of citronellol on oxidative stress, neuroinflammation and autophagy pathways in an in vivo model of Parkinson's disease. *Heliyon* 2022; 8: e11434.
 - 55) Bastin A, Sadeghi A, Nematollahi MH, Abolhasani M, Mohammadi A, Akbari H. The effects of malvidin on oxidative stress parameters and inflammatory cytokines in LPS-induced human THP-1 cells. *J Cell Physiol* 2021; 236: 2790-2799.
 - 56) Decendit A, Mamani-Matsuda M, Aumont V, Waffo-Teguo P, Moynet D, Boniface K, Richard E, Krisa S, Rambert J, Mérillon J-M. Malvidin-3-O-β glucoside, major grape anthocyanin, inhibits human macrophage-derived inflammatory mediators and decreases clinical scores in arthritic rats. *Biochem Pharmacol* 2013; 86: 1461-1467.
 - 57) Abdelsalam RM, Safar MM. Neuroprotective effects of vildagliptin in rat rotenone Parkinson's disease model: role of RAGE-NF κB and Nrf2-antioxidant signaling pathways. *J Neurochem* 2015; 133: 700-707.
 - 58) Zhou Q, Chen B, Wang X, Wu L, Yang Y, Cheng X, Hu Z, Cai X, Yang J, Sun X, Lu W, Yan H, Chen J, Ye J, Shen J, Cao P. Sulforaphane protects against rotenone-induced neurotoxicity in vivo: Involvement of the mTOR, Nrf2, and autophagy pathways. *Sci Rep* 2016; 6: 32206.
 - 59) Fan H, Cui J, Liu F, Zhang W, Yang H, He N, Dong Z, Dong J. Malvidin protects against lipopolysaccharide-induced acute liver injury in mice via regulating Nrf2 and NLRP3 pathways and suppressing apoptosis and autophagy. *Eur J Pharmacol* 2022; 933: 175252.
 - 60) Ahmadi FA, Linseman DA, Grammatopoulos TN, Jones SM, Bouchard RJ, Freed CR, Heidenreich KA, Zawada WM. The pesticide rotenone induces caspase-3-mediated apoptosis in ventral mesencephalic dopaminergic neurons. *J Neurochem* 2003; 87: 914-921.
 - 61) Sari DRT, Safitri A, Cairns JRK, Fatchiyah F. Anti-apoptotic activity of anthocyanins has potential to inhibit caspase-3 signaling. *J Trop Life Sci* 2020; 10: 15-25.
 - 62) Mirza FJ, Zahid S, Amber S, Sumera, Jabeen H, Asim N, Ali Shah SA. Multitargeted Molecu-

- lar Docking and Dynamic Simulation Studies of Bioactive Compounds from *Rosmarinus officinalis* against Alzheimer's Disease. *Molecules* 2022; 27: 7241.
- 63) Sehgal SA, Mannan S, Ali S. Pharmacoinformatic and molecular docking studies reveal potential novel antidepressants against neurodegenerative disorders by targeting HSPB8. *Drug Des Devel Ther* 2016: 1605-1618.
- 64) MD Rizvi S, Shakil S, Biswas D, Shakil S, Shaikh S, Bagga P, A Kamal M. Invokana (Canagliflozin) as a dual inhibitor of acetylcholinesterase and sodium glucose co-transporter 2: advancement in Alzheimer's disease-diabetes type 2 linkage via an enzoinformatics study. *CNS Neurol Disord Drug Targets* 2014; 13: 447-451.
- 65) Shaikh S, Rizvi SMD, Shakil S, Riyaz S, Biswas D, Jahan R. Forxiga (dapagliflozin): Plausible role in the treatment of diabetes-associated neurological disorders. *Biotechnol Appl Biochem* 2016; 63: 145-150.